Supplementary Information

Lignin as precursor of gel electrolyte and salt templated carbon for sustainable electrochemical capacitor

Amelia Klimek[1,2,3,4], Lina Amro[1], Nutthira Pakkang[4,5], Camélia Matei Ghimbeu[2,3,6], Elzbieta Frackowiak*[1], Shiori Suzuki*[4]

[1]Institute of Chemistry and Technical Electrochemistry, Poznan University of Technology, Berdychowo 4, Poznan 60-965, Poland

[2]Institut de Science des Matériaux de Mulhouse, Université de Haute-Alsace, F-68100 Mulhouse, France

[3]Université de Strasbourg, F-67081 Strasbourg, France

[4]Research Faculty of Agriculture, Hokkaido University, Kita 9, Nishi 9, Kita-ku, Sapporo 060-8589, Japan

[5]Department of International Collaborative Program in Sustainable Materials and Technology for Industries between Nagoya University and Chulalongkorn University, Graduate School of Engineering, Nagoya University, Furo-cho, Chikusa-ku, Nagoya 464-8603, Japan

[6]Réseau sur le Stockage Electrochimique de l'Energie (RS2E), 80039 Amiens Cedex, France

*Corresponding authors

elzbieta.frackowiak@put.poznan.pl (EF); suzuki-s@agr.hokudai.ac.jp (SS)

Tab. S1 Summary of the performance of the organic-, aqueous- and lignosulfonate (LS)- based electrochemical capacitors (ECs).

	Organic-based EC	**Neutral aqueous-based EC**	**LS-based EC**
Ionic conductivity	~ 10-50 mS cm^{-1} [1,2]	~ 100 mS cm^{-1} [3]	~ 10 mS cm^{-1}
Voltage range	2.5 V – 3.0 V [4,5]	0.8 V – 1.6 V [6,7]	0.8 V – 1.6 V
Gravimetric capacitance	110 F g^{-1} [8] (1 A g^{-1})	123 F g^{-1} [9] (1 A g^{-1})	100 F g^{-1} (1 A g^{-1})
Energetic efficiency	~ 60-85% [10]	~ 85% [11]	82%
Energy density	~ 30 Wh kg^{-1} [4,5]	~ 20 Wh kg^{-1} [9,12]	~ 10 Wh kg^{-1}
Power density	~ 20 kW kg^{-1} [4,5]	~ 10 kW kg^{-1} [9,12]	~ 30 W kg^{-1}
Leakage current	< 8.0 mA [4]	~ 30 mA g^{-1} [13]	~ 20 mA g^{-1}
Lifetime	1500 h [4] >1 000 000 cycles [4,14]	120 h [13] >100 000 cycles [13]	170 h -
Self-discharge	From 2.7 V to 2.67 V Loss of ~ 3% [15]	From 1.6 V to 0.97 V Loss of ~ 40% [16]	From 1.6 V to 1.1 V Loss of ~ 30%
Assembly	Inert [7]	Air [7]	Air
Safety	Low [7]	Moderate [7]	High
Sustainability	Low [17]	Moderate [17]	High

Tab. S2 Summary of the advantages and disadvantages of the gel electrolytes in the electrochemical capacitors.

Ref.	Device/Type of the gel electrolyte	Advantages	Disadvantages
[18]	Flexible supercapacitor ($NaClO_4$ + PVA)	- Electrolyte leakage is reduced - Temperature robustness up to 80°C	- Lower ionic conductivity of gel than for liquid electrolyte solution (difference of 10 mS cm^{-1})
[19]	Supercapacitor (KOAc + gelatin/glycerol, NaCl + gelatin/glycerol)	- Combination of EDL formation and faradaic reactions - Increased ion adsorption at the electrode/electrolyte interface	- Decrease of ionic conductivity and mobility of Na^+ and CH_3COO^- within the gel structure
[20]	Supercapacitor (KOH + chitosan/glyoxylic acid)	- Good mechanical properties - Better capacitance retention than liquid electrolyte - Inhibiting corrosion issues in the cell	- Low ionic conductivity - The gel electrolyte requires ~2 days of aging before it becomes mechanically exploitable - Limited voltage (0.8 V)
[21]	Flexible supercapacitor (KOH + alkali lignin/PVA/PEGDGE)	- High ionic conductivity and mechanical integrity (10 mS cm^{-1}) - Flexibility and durability of the crosslinked gel network	- Limited voltage of the system due to use of aqueous based medium
[22]	Supercapacitor (KOH + lignin/PEGDGE)	- High swelling capacity - Flexibility confirmed by stable capacitance under bending and twisting	- Low ionic conductivity - Voltage limitation (up to 1.0 V)
[23]	Supercapacitor (LiOAc + Lithium alginate; LiOAc + PVA)	- Flame retardant performance (oxygen index of 35%) - High ionic conductivity (33 mS cm^{-1}) - High operating voltage of 1.8 V	- Reduced mechanical strength at high salt concentration

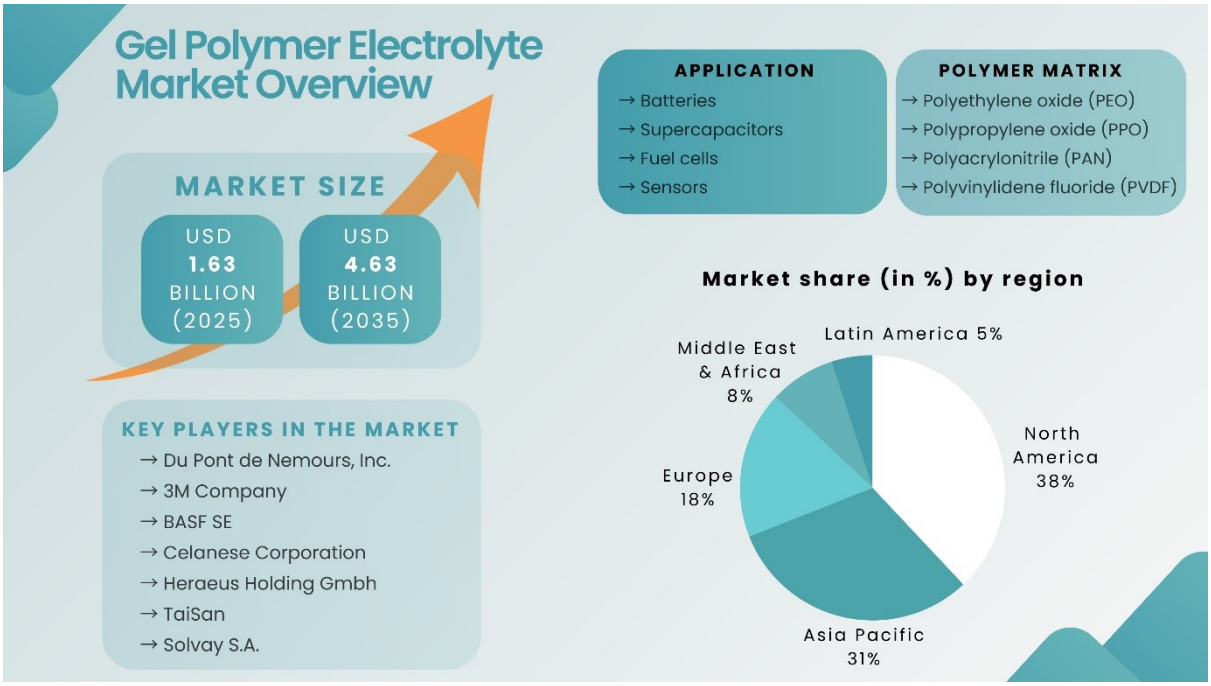

Fig. S1 Schematic diagram of the current and the future demand and supply of the gel electrolytes (data extracted from ref[24]).

Tab. S3 Summary of the type/example of the polymer used in the gel electrolyte and its climate change potential (CPP) and cumulative energy demanded (CED).

Type of the polymer used in the gel electrolyte	**Example of the polymer used in the gel electrolyte**	**Climate change potential (CCP) (kg CO_2-eq / kg of polymer)**	**Cumulative energy demand (CED) (MJ / kg)**
Petrochemical-based	Polyvinylidene fluoride (PVDF)	55.80 [25]	756 [25]
	Polyacrylonitrile (PAN)	10.64 [26]	245 [27]
Biomass-based	Silk fibroin	1.30 [28]	1843 [29]
Biopolymer-based	Sodium lignosulfonate	3.23 [28]	48.8 [30]
	Kraft lignin	2.80 [28]	31.5 [31]
	Cellulose pulp	0.21 [28]	93 [32]

Tab. S4 Quantities of hydroxyl and carboxylic groups in mmol g^{-1} calculated using ^{31}P NMR analysis.

Sample	Quantity (mmol g^{-1})			
	Aliphatic -OH	**Aromatic -OH**	**Carboxylic-COOH**	**Total -OH**
LS	2.62	1.53	0.31	4.46

Tab. S5 Composition ratios of lignosulfonate (LS) / crosslinker (PEGDGE) – based gels.

Mn PEGDGE (g / mol)	**g PEGDGE / g LS**	**PEGDGE wt.% in the gel**	**LS wt.% in the gel**	**mmol PEGDGE / g LS**	**mmol epoxy / mmol OH total of LS**
1099	0.4	28	72	0.36	0.17

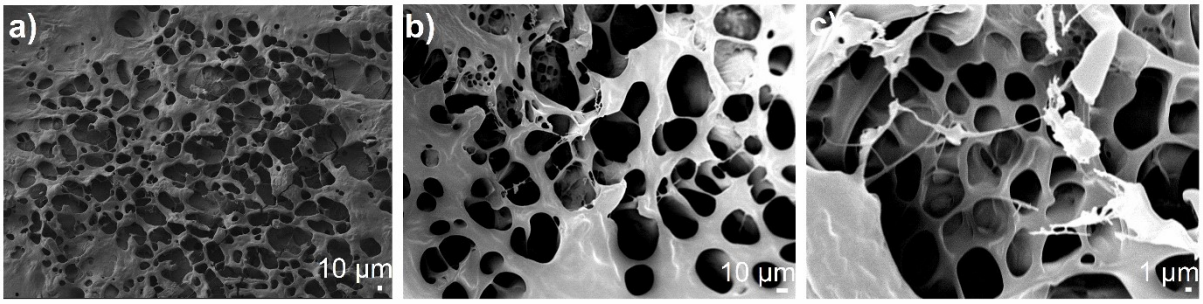

Fig. S2 a-c) Cryo SEM images of LS hydrogel.

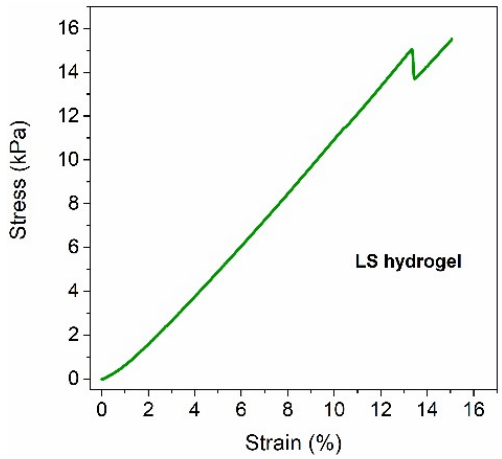

Fig. S3 Compression test result of LS hydrogel.

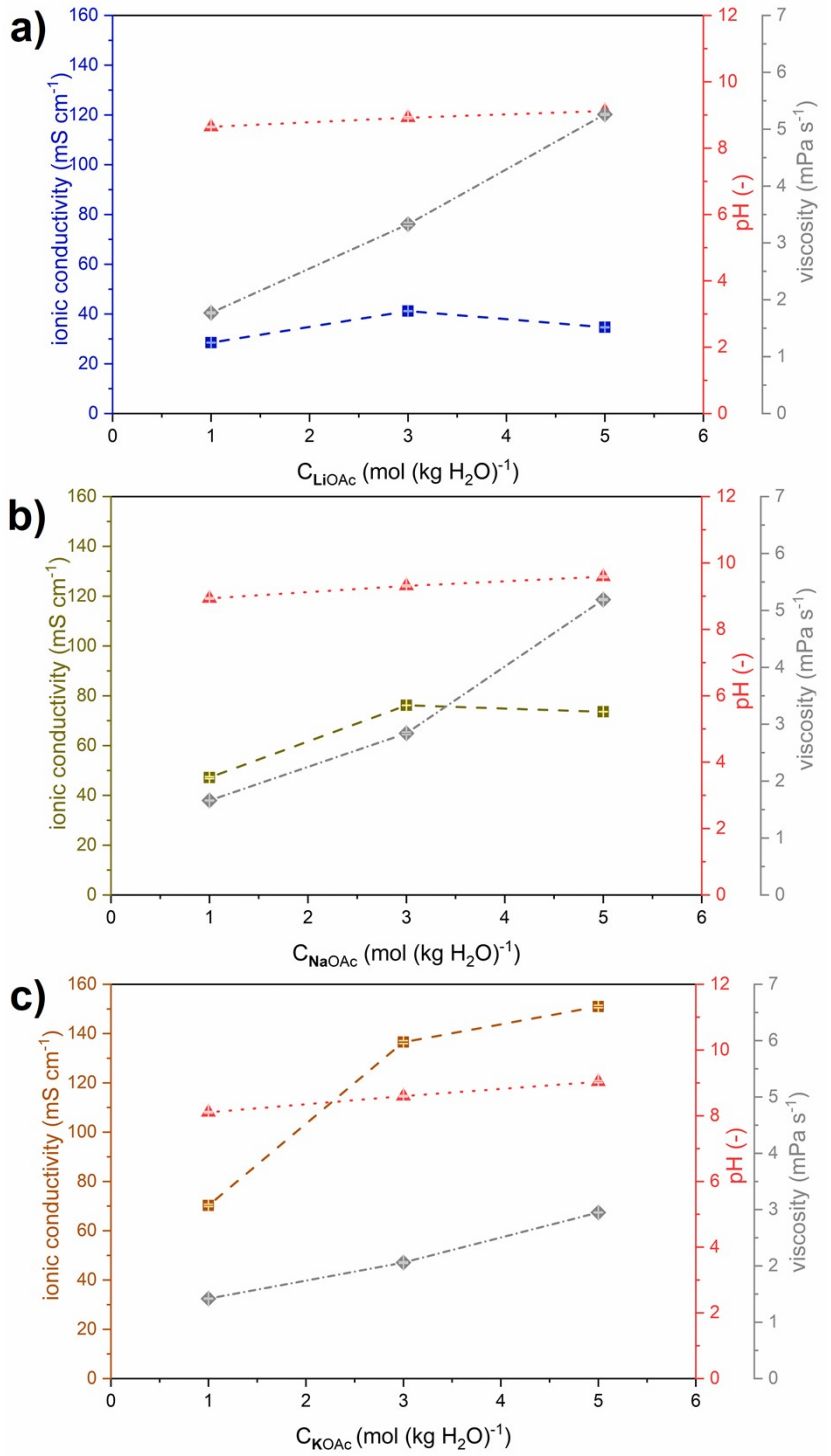

Fig. S4 Physicochemical characterization (ionic conductivity, pH, and viscosity) of selected aqueous electrolytes in different concentrations 1, 3, and 5 m: **a)** LiOAc, **b)** NaOAc, **c)** KOAc.

Tab. S6 Selected thermodynamic and physical characteristics of ions used in the preparation of gel electrolytes and synthesis of salt templated carbons for ECs testing[33–38].

Ion	Crystal ionic diameter (nm)	Hydrated ion diameter (nm)	Hydration enthalpy (-kJ mol^{-1})	Binding energy (kcal mol^{-1})	Ion mobility (10^{-8} m^2 s^{-1} V^{-1})
Li^+	0.152	0.680	520	38	4.01
Na^+	0.232	0.598	406	28	5.20
K^+	0.304	0.662	322	19	7.60

Tab. S7 Selected mass concentrations and molalities of potassium acetate (KOAc).

Molality mol (kg H_2O)$^{-1}$	Mass concentration (%)
1	9
3	23
5	33
7	41
10	50
11	51
15	60
19	65
24	70

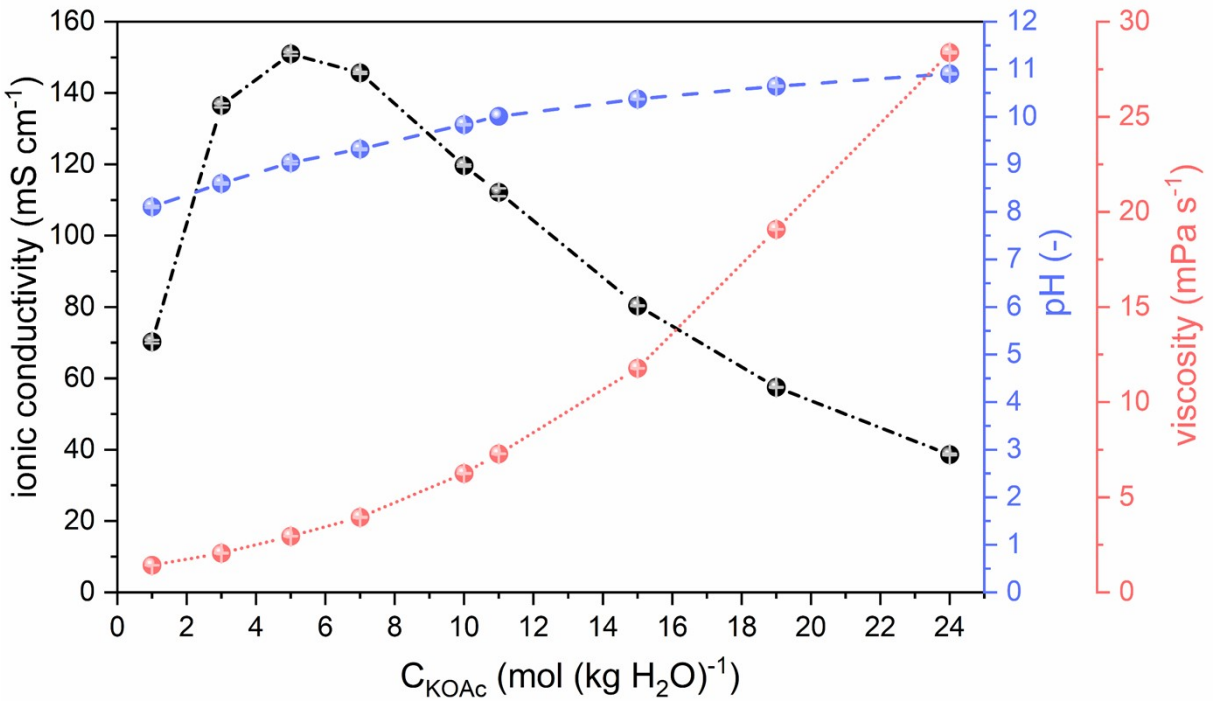

Fig. S5 Physicochemical characterization (ionic conductivity, pH, and viscosity) of KOAc in different concentrations (1 – 24 m).

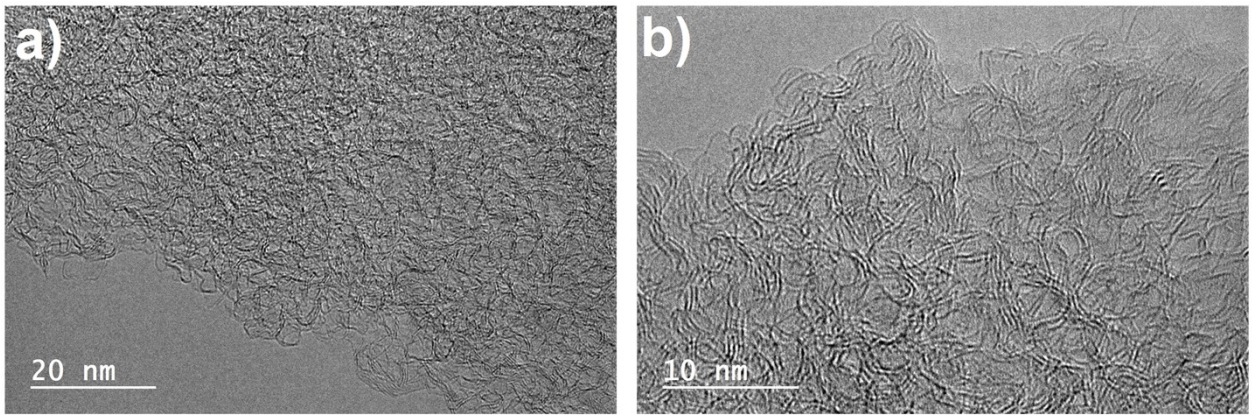

Fig. S6 a-b) HRTEM images of YP80F commercial carbon using different scales.

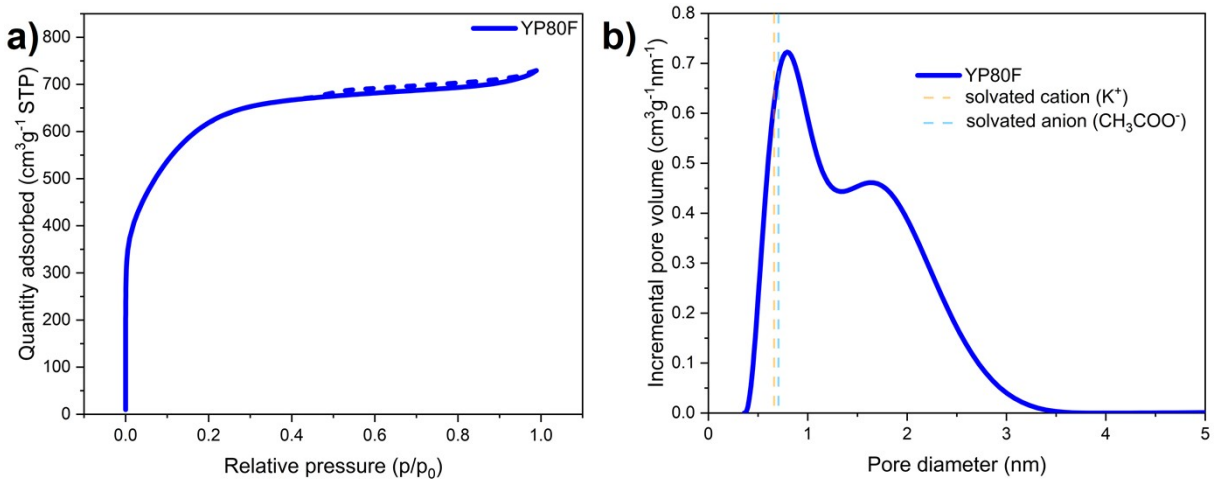

Fig. S7 a) Nitrogen sorption at 77K and **b)** pore size distribution of the YP80F commercial carbon. The vertical dash lines present solvated ion diameter of cation (K^+) and anion (OAc^-).

Tab. S8 Textural properties of YP80F activated carbon determined by nitrogen sorption: specific surface area (S_{BET}, S_{DFT}), C value of BET, volume of micropores (V_{micro}), volume of mesopores (V_{meso}), average diameter of micropores ($L_{0\ micro}$), average diameter of mesopores ($L_{0\ meso}$) and Raman I_{D1}/I_G ratio.

carbon	**S_{BET} ($m^2\ g^{-1}$)**	**C value**	**S_{DFT} ($m^2\ g^{-1}$)**	**V_{micro} ($cm^3\ g^{-1}$)**	**V_{meso} ($cm^3\ g^{-1}$)**	**$L_{0\ micro}$ (nm)**	**$L_{0\ meso}$ (nm)**	**I_{D1}/I_G**
YP80F	2018 ±31	332	1666	0.78	0.24	1.03	2.86	2.50

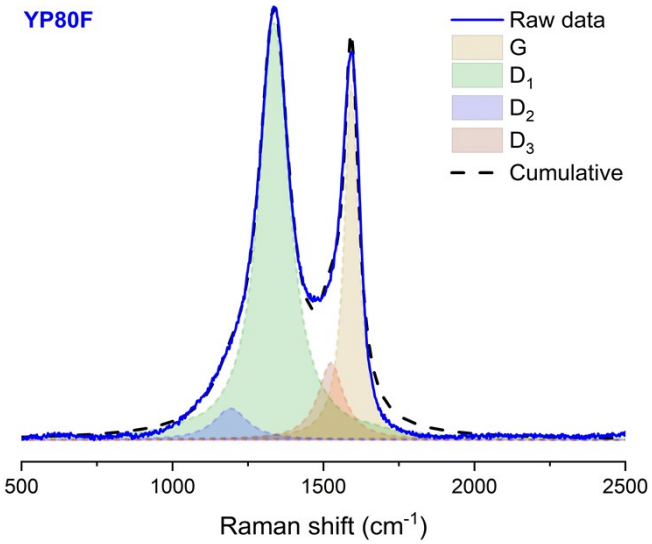

Fig. S8 Raman spectra deconvoluted into four peaks using Lorentzian fitting function of commercial carbon (YP80F).

Tab. S9 Elemental analysis results of LS-carbons (CLS-SA, CLS-NaOAc, CLS-KOAc, CLS-NaKOAc) and commercial carbon (YP80F).

Carbon	**C wt.%**	**H wt.%**	**N wt.%**	**S wt.%**	**O wt.%**	**Total heteroatoms wt.%**
CLS-SA	87.4	0.7	0.2	0.2	6.0	7.1
CLS-NaOAc	85.0	0.3	0.8	0.1	6.7	7.9
CLS-KOAc	85.5	0.3	0.3	0.3	7.5	8.4
CLS-NaKOAc	86.8	0.4	0.1	0.9	5.0	6.4
YP80F	94.6	0.5	0.1	0.0	1.9	2.5

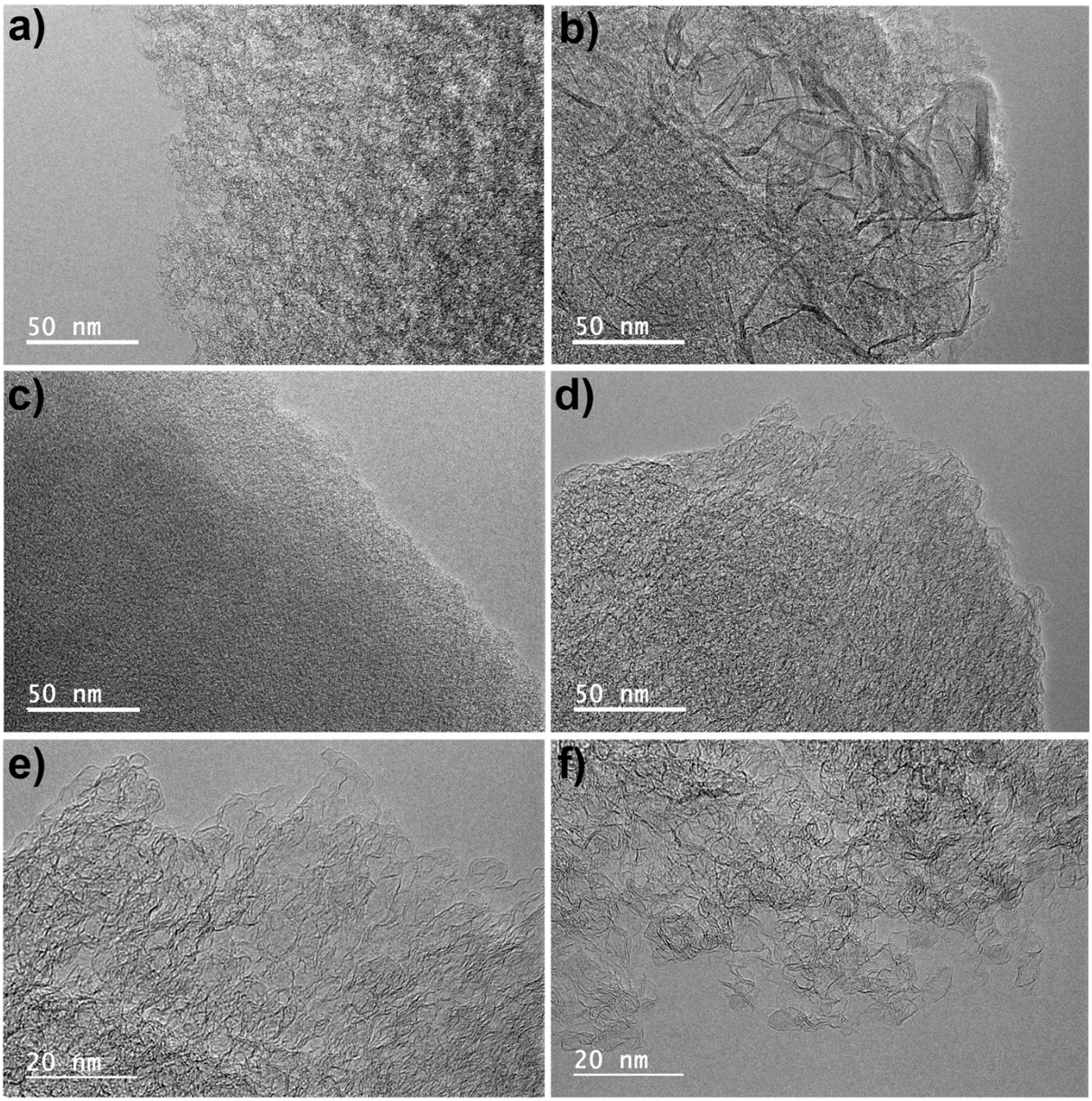

Fig. S9 HRTEM images of LS-carbons: **a)** CLS-SA, **b)** CLS-NaOAc, **c)** CLS-KOAc, **d-f)** CLS-NaKOAc.

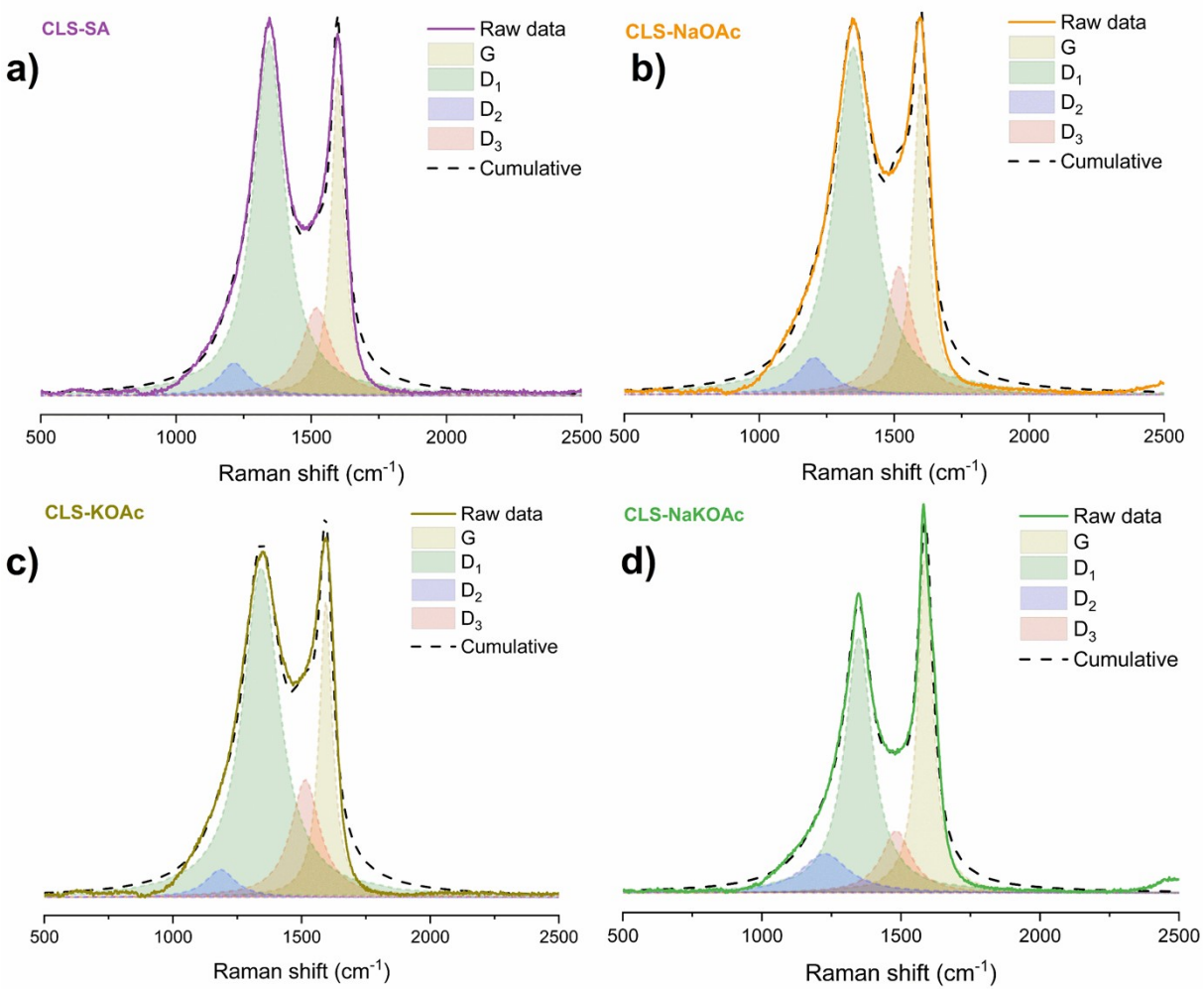

Fig. S10 Raman spectra deconvoluted into four peaks using Lorentzian fitting function of: **a)** CLS-SA, **b)** CLS-NaOAc, **c)** CLS-KOAc, **d)** CLS-NaKOAc carbons.

Tab. S10 Summary of the size (height) of stacked graphene layers (La) and I_{D1}/I_G area ratio after two peaks fitting of salt templated carbons.

Carbon	**La (nm)**	**I_{D1}/I_G**
CLS-SA	6.42	2.61±0.07
CLS-NaOAc	5.96	2.81±0.01
CLS-KOAc	5.58	3.00±0.09
CLS-NaKOAc	12.33	1.37±0.05

Tab. S11 Textural properties of LS-carbons determined by nitrogen sorption: specific surface area (S_{BET}, S_{DFT}), C values of BET, volume of micropores (V_{micro}), volume of mesopores (V_{meso}), average diameter of micropores ($L_{0\ micro}$), average diameter of mesopores ($L_{0\ meso}$).

Carbon	S_{BET} ($m^2\ g^{-1}$)	C value	S_{DFT} ($m^2\ g^{-1}$)	V_{micro} ($cm^3\ g^{-1}$)	V_{meso} ($cm^3\ g^{-1}$)	$L_{0\ micro}$ (nm)	$L_{0\ meso}$ (nm)
CLS-SA	1079±10	462	965	0.35	0.38	1.06	4.29
CLS-NaOAc	881±2	839	825	0.31	0.05	0.79	3.20
CLS-KOAc	1754±6	746	1587	0.63	0.05	0.79	2.88
CLS-NaKOAc	1169±5	454	1035	0.42	0.18	0.85	4.08

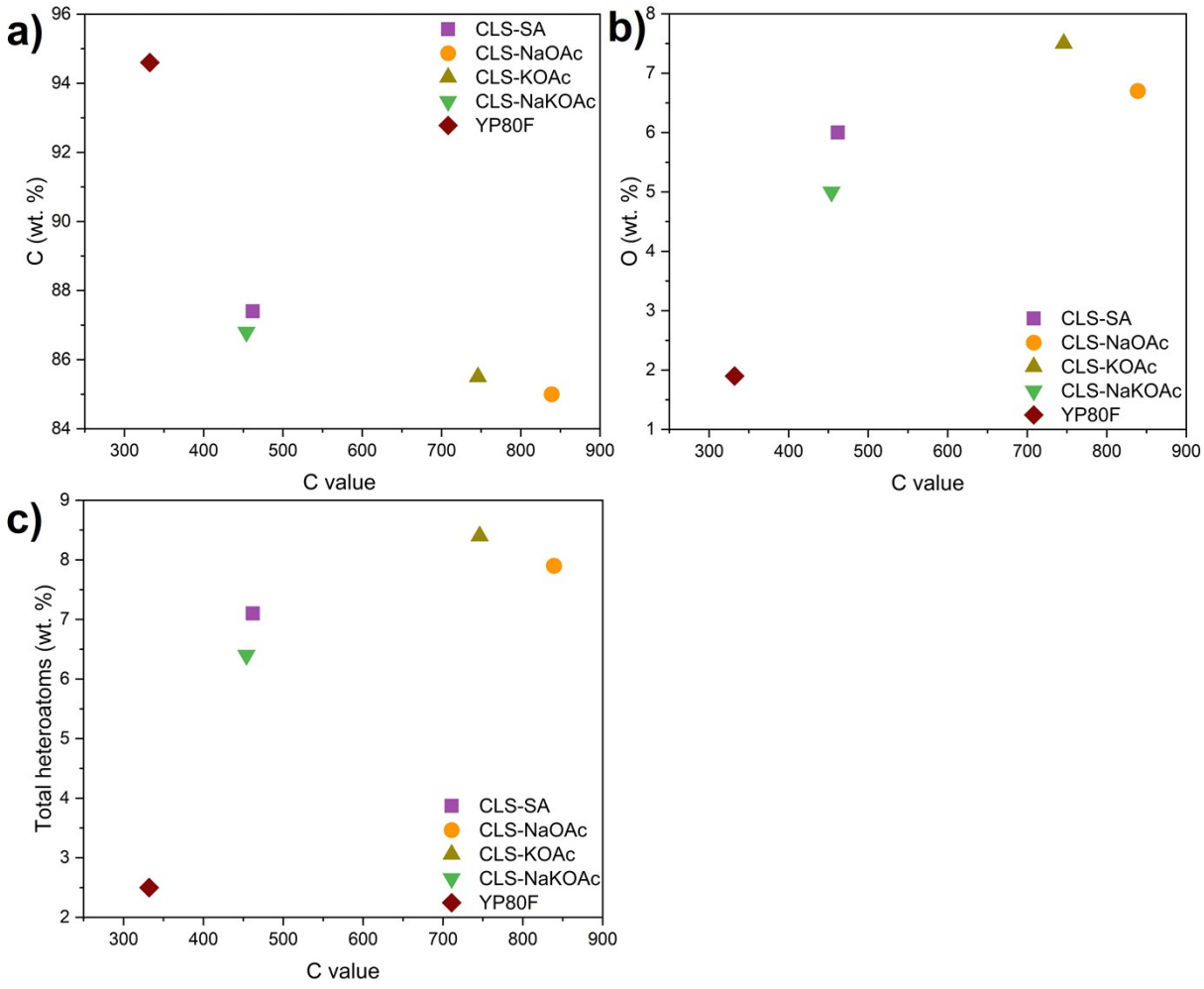

Fig. S11 Plots of C value and: **a)** C wt. %, **b)** O wt.%, **c)** total heteroatoms wt.%.

Tab. S12 Textural properties of LS-carbons determined by nitrogen sorption: specific surface area (S_{BET}), volume of micropores (V_{micro}), volume of mesopores (V_{meso}), average diameter of micropores ($L_{0\ micro}$), average diameter of mesopores ($L_{0\ meso}$) and Raman I_{D1}/I_G ratio.

carbon	S_{BET} ($m^2\ g^{-1}$)	V_{micro} ($cm^3\ g^{-1}$)	V_{meso} ($cm^3\ g^{-1}$)	$L_{0\ micro}$ (nm)	$L_{0\ meso}$ (nm)	I_{D1}/I_G
CLS-NaKOAc (1:1)	1169±5	0.42	0.18	0.85	4.08	1.37
CLS-NaKOAc (2:1)	752±1	0.27	0.04	0.75	3.60	1.80

Tab. S13 Reported gravimetric capacitance values of LS-based ECs operating in LS–5 m KOAc GE.

1.6 V / LS	CLS-SA	CLS-NaOAc	CLS-KOAc	CLS-NaKOAc
Current density ($A\ g^{-1}$)	Gravimetric capacitance ($F\ g^{-1}$)			
0.1	81±1	77±1	119±4	82±5
0.2	77±2	67±1	108±3	72±3
0.5	63±4	46±6	82±1	52±3
1	48±4	29±4	58±4	29±2
2	27±4	9±5	28±4	9±4

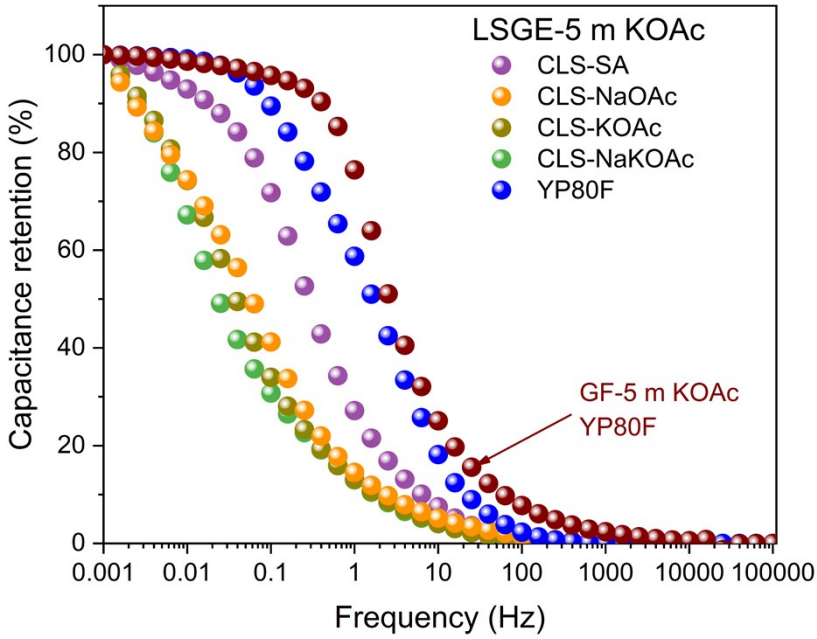

Fig. S12 Capacitance retention *vs.* frequency of LS-carbons-based ECs and commercial carbon YP80F operating in LS-5 m KOAc GE at 1.6 V.

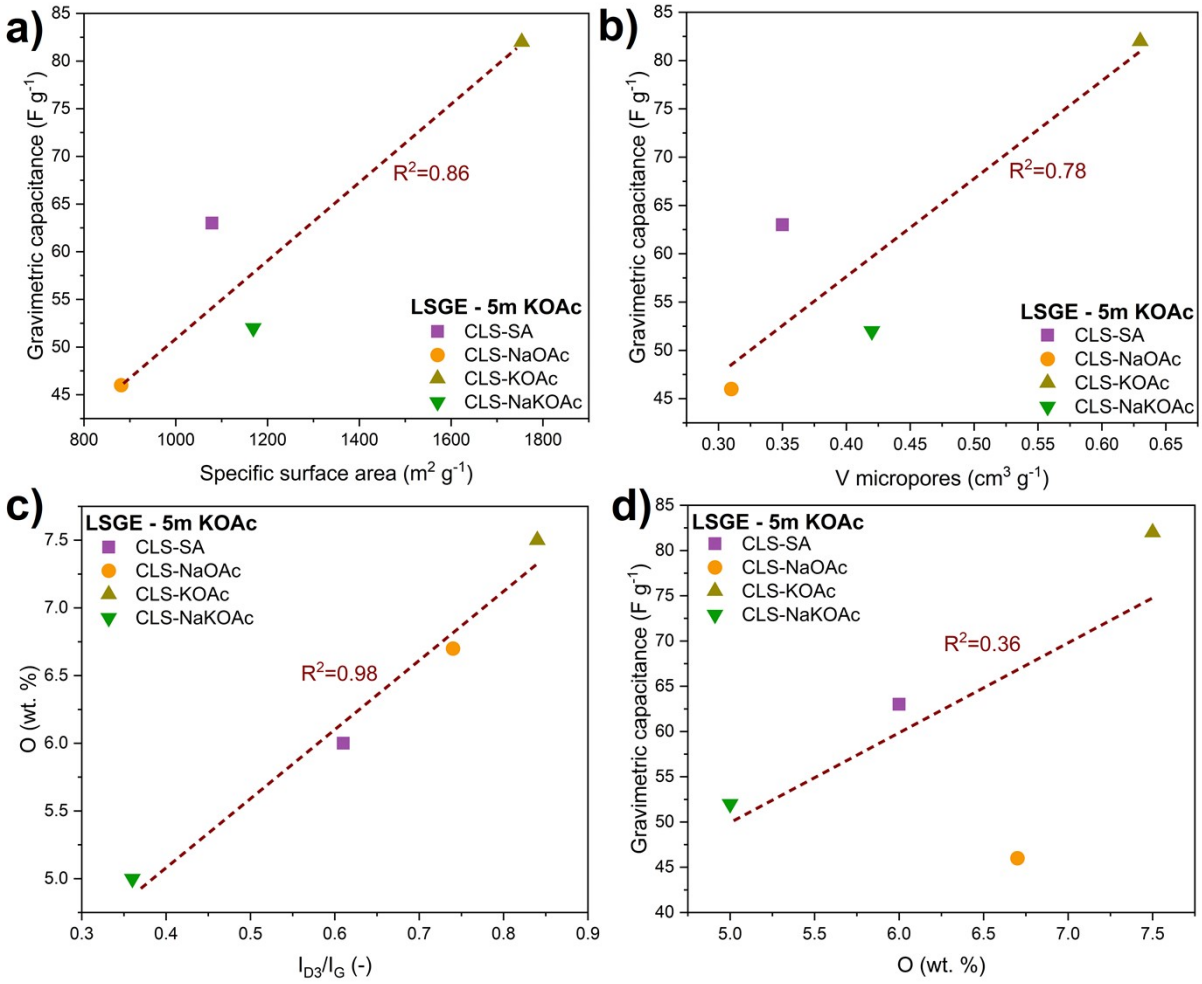

Fig. S13 Correlation of: **a)** specific surface area *vs.* gravimetric capacitance (0.5 A g^{-1}), **b)** volume of micropores *vs.* gravimetric capacitance (0.5 A g^{-1}), **c)** I_{D3}/I_G *vs.* total amount of oxygen in wt.%, **d)** total amount of oxygen in wt.% *vs.* gravimetric capacitance (0.5 A g^{-1}).

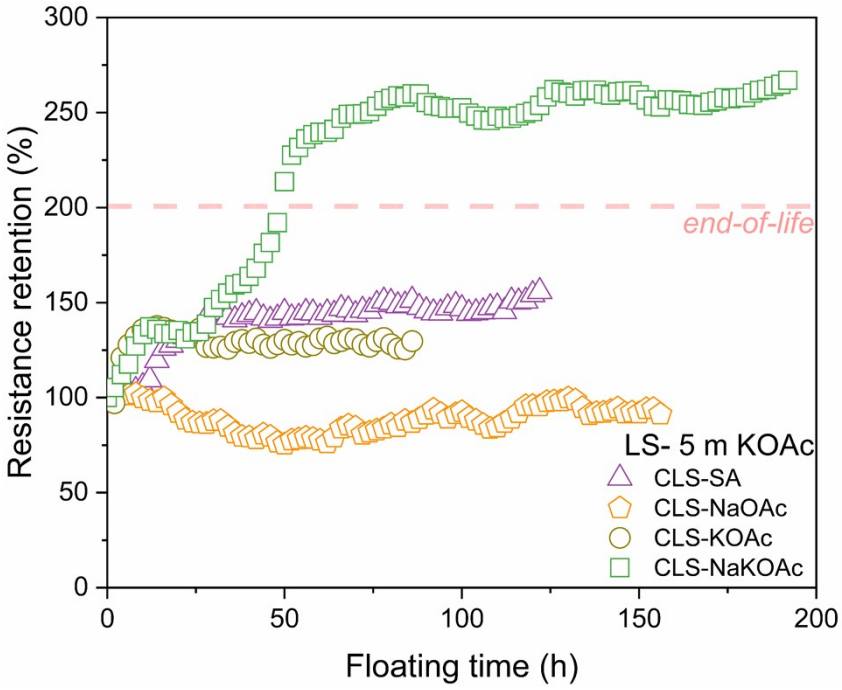

Fig. S14 Relative resistance *vs.* floating time of LS-carbons-based ECs operating in LS-5 m KOAc GE at 1.6 V.

Tab. S14 Summary of the electrochemical performance of ECs.

Electrode material	**Specific surface area**	**Electrolyte**	**Gravimetric capacitance**	**Lifespan**	**Ref.**
Salt templated carbon (KOAc/LS)	1754 m^2 g^{-1}	PEGDGE/LS + 5 m KOAc gel electrolyte	82 F g^{-1} at 0.5 A g^{-1} (1.6 V)	52 h of floating at 1.6 V	***This work***
Salt templated carbon (NaKOAc/LS)	1169 m^2 g^{-1}	PEGDGE/LS + 5 m KOAc gel electrolyte	52 F g^{-1} at 0.5 A g^{-1} (1.6 V)	170 h of floating at 1.6 V	***This work***
Spinning of lignin/PAN	1176 m^2 g^{-1}	PEGDGE/lignin + 3.3 M KOH gel electrolyte	129 F g^{-1} at 0.5 A g^{-1} (1.0 V)	10,000 cycles (95%)	[21]

Carbonization of aerogel prepared from organosolv lignin/PEGDGE	-	PEGDGE/Organosolv lignin + 6 M KOH gel electrolyte	41 F g^{-1} at 0.5 A g^{-1} (1.0 V)	-	22
Carbon cloth activated by H_2SO_4 and HNO_3	-	Sodium alginate/Aspartic acid-modified lignin hydrogel	40 F g^{-1} at 0.5 A g^{-1} (1.0 V)	-	39
Activated carbon	-	PEGDGE/Gelatin/ lignin + 3.3 M KOH gel electrolyte	145 F g^{-1} at 0.5 A g^{-1} (1.0 V)	6,000 cycles (81%)	40
Activated carbon (commercial YP80F)	2093 m^2 g^{-1}	Gelatin/Glycerol + 2.5 M CH_3COONa	75 F g^{-1} at 0.5 A g^{-1} (1.0 V)	50,000 cycles (61%)	19
Activated carbon (commercial Norit R3)	1249 m^2 g^{-1}	$FeCl_3$/Chitosan + 2 M KOH	76 F g^{-1} at 0.5 A g^{-1} (0.8 V)	10,000 cycles (89%)	20

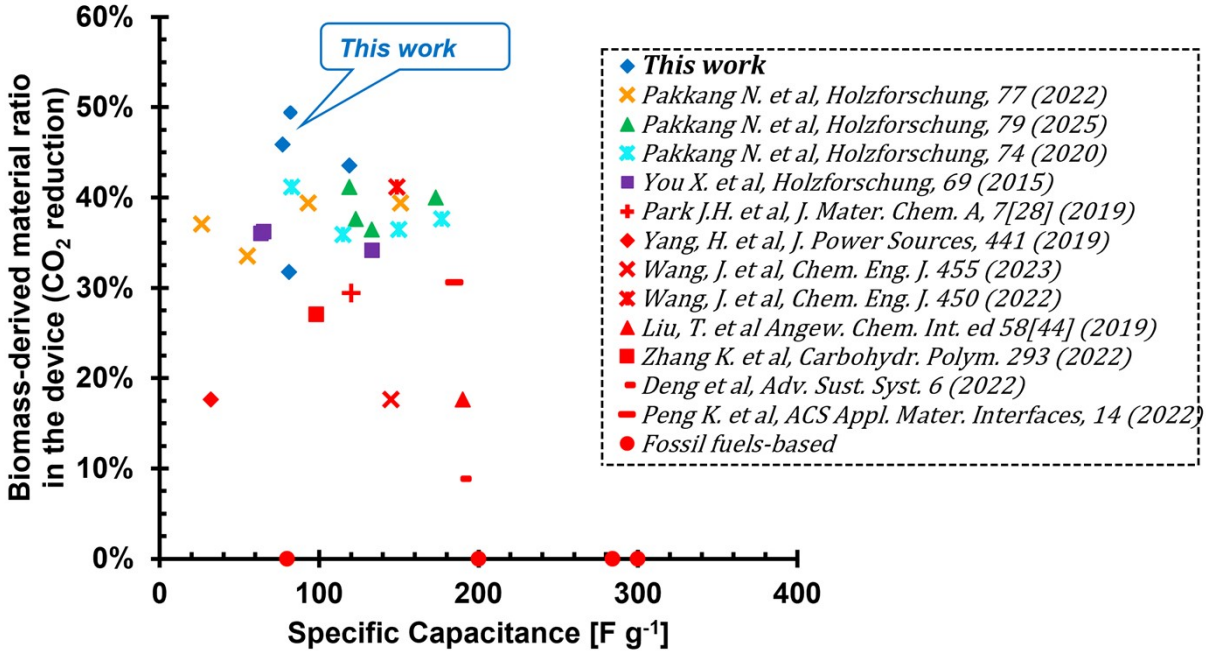

Fig. S15 Biomass-derived material ratio in the device (CO_2 reduction) *vs.* specific capacitance based on references [21,40–51].

References

1 Z. Bo, X. Zhang, Z. Huang, Y. Huang, J. Yan, K. Cen and H. Yang, *RSC Adv.* 2023, **13**, 15762–15771.

2 M. Gasko, I.M. Patil, L. Kops, D. Kruger, C. Neumann, A. Turchanin, F. A. Kreth and A. Balducci, Batteries&Supercaps, 2024, **7**, e202400283.

3 X. Zang, C. Shen, M. Sanghadasa and L. Lin, *ChemElectroChem,* 2019, **6**, 954–954.

4 SkelCap Supercapacitor, Skeleton Technologies GmbH, Preliminary Data Sheet, 2024.

5 K. Dissanayake and D. Kularantna-Abeywardana, *J.Energy Storage*, 2024, **96**, 112563.

6 K. Fic, A. Płatek, J. Piwek, J. Menzel, A. Ślesiński, P. Bujewska, P. Galek, and E. Frąckowiak, *Energy Storage Mater.,* 2019, **22**, 1–14.

7 S. Azmi, A. Klimek, E. Frackowiak, *Electrochim. Acta,* 2023, **452**, 142347.

8 B.S. Mao, Z. Wen, Z. Bo, J. Chang, X. Huang and J. Chen, *ACS Appl. Mater. Interfaces,* 2014, **6**, 9881-9889.

9 M.P. Bichat, E. Raymundo-Piñero and F. Béguin, *Carbon* 2010, **48**, 4351–4361.

10 R. Chen, D. Bresser, M. Saraf, P. Gerlach, A. Balducci, S. Kunz, D. Schroder, S. Passerini and J. Chen, *ChemSusChem*, 2020, **13**, 2205-2219.

11 A. Platek, C. Nita, C. Matei Ghimbeu, E. Frąckowiak and K. Fic, *Electrochim. Acta,* 2020, **338**, 135788.

12 D. Zhang, B. Yang, W. She, S. Gao, J. Wang, Y. Wang, K. Wang, H. Li and L. Han, *J. Power Sources,* 2021, **506**, 230103.

13 N. Fechler, T.P. Fellinger and M. Antonietti, *Adv. Mater.*, 2013, **25**, 75–79.

14 B. Pal, S. Yang, S. Ramesh, V. Thangadurai and R. Jose, *Nanoscale Adv.,* 2019, **1**, 3807–3835.

15 J. Kowal, E. Avaroglu, F. Chamekh, A. Šenfelds, T. Thien, D. Wijaya and D.U. Sauer, *J. Power* Sources, 2011, **196**, 573–579.

16 P. Galek, A. Slesinski, K. Fic and J. Menzel, *J. Mater. Chem. A*, 2021, **9**, 8644-8654.

17 X. Ma, D. Zhang, J. Wen, L. Fan, A.M. Rao and B. Lu, *Chem. Eur. J.*, 2024, **30**, e202400332.

18 K. Gong, H. Lee, Y. Choi, G. Jung, K. Keum, J.W. Kim and J.S. Ha, *Electrochim. Acta,* 2024, **475**, 143585.

19 G. Landi, L. La Notte, V. Granata, G. Avallone, C. Barone, G. Carapella and S. Pagano, *ChemElectroChem*, 2023, **10**, e202300443.

20 S. Zallouz, J.M. Le Meins and C. Matei Ghimbeu, *Energy Adv.,* 2022, **1**, 1051-1064.

21 J.H. Park, H.H. Rana, J.Y. Lee and H.S. Park, *J. Mater. Chem. A*, 2019, **7**, 16962-16968.

22 M. Muddasar, A. Beaucamp, M. Culebras and M.N. Collins, *Mater. Today Sustain.,* 2024, **26**, 100767.

23 T. Ye, D. Li, H. Liu, X. She, Y. Xia, S. Zhang, H. Zhang and D. Yang, *Macromolecules,* 2018, **51**, 9360–9367.

24 Research Nester, “Gel Polymer Electrolyte Market - Size, Emerging Trends & Forecast to 2035.

25 X. Hu, A.K.J. An and S.S. Chopra, *ACS Sustainable Chem. Eng*., 2022, **10**, 5708-5718.

26 A. Larrabide, I. Rey and E. Lizundia, *Adv. Energy Sustain. Res.*, 2022, **3**, 2200079.

27 A. Dér, N. Dilger, A. Kaluza, C. Creighton, S. Kara, R. Varley, C. Herrmann and S. Thiede, *J. Clean. Prod.,* 2021, **303**, 127105.

28 J. Huang, S. Wang, J. Chen, C. Chen, E. Lizundia, *Adv. Mater.,* 2025, **37**, 2416733.

29 F. Vollrath, R. Carter, G. K. Rajesh, G. Thalwitz and M. F. Astudillo, Life Cycle Analysis of Cumulative Energy Demand on Sericulture in Karnataka, India, BISERICA 2013 6th BACSA International Conference: Building Value Chains in Sericulture.

30 Borregaard USA, Inc., Environmental Product Declaration: Sodium Lignin Biopolymer D

Powder, NEPD-5614-4920-EN, The Norwegian EPD Foundation, 2023.
31 M. Lettner, P. Solt, B. Rößiger, D. Pufky-Heinrich, A.S. Jääskeläinen, P. Schwarzbauer and F. Hesser, *Sustainability*, 2018, **10**, 2745.
32 T. Hammar, D. Peñaloza, A.C. Hanning, N. Haatanen and J. Pakkasmaa, *J. Clean. Prod.,* 2023, **426**, 139189.
33 M.V. Fedotova and S.E. Kruchinin, *J. Mol. Liq.,* 2011, **164**, 201–206. 34
34 H.D.B. Jenkins and K.P. Thakur, *J. Chem. Educ.,* 1979, **56**, 576.
35 A. Platek-Mielczarek, C. Nita, C. Matei Ghimbeu, E. Frackowiak, and K. Fic, *ACS Appl. Mater. Interfaces,* 2021, **13**, 2584–2599.
36 C. Nita, M. Bensafia, C. Vaulot, L. Delmotte and C. Matei Ghimbeu, *Carbon,* 2016, **109**, 227–238.
37 R. Ludwig, *Angew. Chem. Int. Ed.,* 2001, **40**, 1808–1827.
38 Y. Marcus Chapter 3, Solvents for ions, in Ions in solution and their solvation, 2015. https://onlinelibrary.wiley.com/doi/10.1002/9781118892336.ch3
39 H.F. Wan, X. Zhao, Q. Guo, C. Gao and R.C. Sun, *Front. Chem. Sci. Eng.,* 2025, **19**, 34.
40 J. Wang, C. Gao, P. Hou, Y. Liu, J. Zhao and P. Huo, *Chem. Eng. J.,* 2023, **455**, 140952.
41 N. Pakkang, S. Suzuki, K. Shigetomi and Y. Uraki, *Holzforschung,* 2023, **77**, 119–126.
42 N. Pakkang, M. Hori, S. Suzuki and Y. Uraki, *Holzforschung,* 2025, **79**, 168–176.
43 N. Pakkang, M. Kumar, S. Taira, K. Koda, K. Shigetomi and Y. Uraki, *Holzforschung*, 2020, **74**, 577–588.
44 H. Yang, X. Ji, Y. Tan, Y. Liu and F. Ran, *J. Power Sources,* 2019, **441**, 227174.
45 Y. Wang, N. Chen, Y. Liu, X. Zhou, B. Pu, Y. Qing, M. Zhang, X. Jiang, J. Huang, Q. Tang, B. Zhou and W. Yang, *Chem. Eng. J.,* 2022, **450**, 138398.
46 Y. Wang, F. Chen, Z. Liu, Z. Tang, Q. Yang, Y. Zhao, S. Du, Q. Chen and C. Zhi, *Angew. Chem. Int. Ed.,* 2019, **58**, 15707–15711.
47 K. Zhang, Y. Pang, C. Chen, M. Wu, Y. Liu, S. Yu, L. Li, Z. Ji and J. Pang, *Carbohydr. Polym.,* 2022, **293**, 119673.
48 Y. Deng, H. Wang, K. Zhang, J. Qiu and L. Yan, *Adv. Sustain. Syst.,* 2022, **6**, 2100191.
49 K. Peng, J. Zhang, J. Yang, L. Lin, Q. Gan, Z. Yang, Y. Chen and C. Feng, *ACS Appl. Mater. Interfaces,* 2022, **14**, 39404–39419.
50 X. You, K. Koda, T. Yamada and Y. Uraki, *Holzforschung,* 2015, **69**, 1097–1106.
51 S.M. Benoy, A. Hazarika, M. Rajbongshi, D. Sarmah, M.K. Phukan and B.K. Saikia, *ACS Appl. Energy Mater.,* 2024, **7**, 6045-6061.